Electrical manifestation of the quantum-confined Stark effect by quantum capacitance response in an optically excited quantum well

Yan Tang,* Houzhi Zheng, Fuhua Yang, Pingheng Tan, Chengfang Li, and Yuexia Li
National Laboratory for Superlattices and Microstructures, Institute of Semiconductors, Chinese Academy of Sciences, P. O. Box 912, Beijing 100083, People's Republic of China
(Received 7 December 2000; published 28 February 2001)

We have studied the capacitance-voltage characteristics of an optically excited wide quantum well. Both self-consistent simulations and experimental results show the striking quantum contribution to the capacitance near zero bias which is ascribed to the swift decreasing of the overlap between the electron and hole wave functions in the well as the longitudinal field goes up. This quantum capacitance feature is regarded as an electrical manifestation of the quantum-confined Stark effect.

DOI: 10.1103/PhysRevB.63.113305 PACS number(s): 73.21.−b, 71.70.Ej, 84.37.+q, 85.60.Gz

It is well known that the capacitance characteristics of low-dimensional semiconductor heterostructures are of substantial importance both in fundamental research and in device applications. On the one hand, capacitance measurements in such systems display various important physical phenomena that are related to the carrier confinements;[1–5] on the other hand, capacitance knowledge also helps one to exploit practical applications of semiconductor quantum structures like high-speed electronic and optoelectronic devices.[6–11]

The capacitance-voltage (C-V) characteristics of low-dimensional structures are in general strongly nonlinear, and show clear fingerprints of quantum confinement, which is therefore referred to so-called *quantum capacitance*. The conception of quantum capacitance was first introduced by Luryi for describing the property of a two-dimensional Fermi system in a gated quantum well (QW).[12] Many other researchers investigated quantum capacitance in various quantum structures, including double-barrier resonant-tunneling structures,[6–11] superlattice structures,[13] interband tunneling structures,[14] quantum dots (QD's),[1–4] and δ-doped structures.[15] For gated structures like the gated QW proposed by Luryi, or QD's embedded in a metal-insulator-semiconductor field-effect transistor structure, the meaning of the quantum capacitance can be inferred from its relevance to the characteristic density of states (two dimensional or zero dimensional respectively). In tunneling structures, the quantum contribution to the total capacitance is a consequence of the variation of the wave function under different applied biases, and is more directly related to the nature of the quantum size effect. However, it should be pointed out that only the quantum nature of a single type of carrier, usually electrons, has been concerned in the abovementioned structures.

In our present work, C-V measurement under optical excitation offers us the opportunity of observing a type of quantum capacitance associated with both electron and hole wave function features in a wide QW. As predicted by self-consistent simulations, and then demonstrated by experimental results, a sharp capacitance peak grows near zero bias with the photoexcitation, in response to a quick decreasing of the overlap between the electron and hole envelope functions as the applied bias goes up either positively or negatively. That is substantially different from the classical electric polarization effect, where electrons and holes are regarded as classically charged particles separately dwelling in certain spatial locations. On this account, the capacitance feature we describe here is a type of quantum capacitance, and is actually an electrical manifestation of the *quantum-confined Stark effect*, which is usually detectable only by means of optical spectroscopies (e.g., photoluminescence, absorption, or transmission spectra).

The system under investigation is a symmetric n^+-i-n^+ double-barrier structure (DBS) grown by molecular beam epitaxy on a (100)-oriented n^+-GaAs substrate. The layer sequence is as follows: a 2-μm GaAs buffer layer, Si doped to 10^{18}cm^{-3}; a 50-nm undoped GaAs spacer; a 25-nm undoped AlAs barrier; a 63.5-nm undoped GaAs well; a 25-nm undoped AlAs barrier; a 50-nm undoped GaAs spacer; and a 100-nm GaAs cap layer, Si doped to 10^{18}cm^{-3}. The conduction band-edge of the DBS is schematically profiled in Fig. 1 (a). Employing a nontransparent thick barrier brings us two advantages: first, we can optically inject a controlled number of electrons and holes into the QW; second, it facilitates the analysis of our system.[9,10] There is no doubt that the central well, as a whole, must keep neutrality because optical excitation creates equal amounts of electrons and holes. Under biases, the negative charges ($-Q_s$) stored in the accumulation region (I) are well separated from the positive charges (Q_s) in the depletion region (III) by a wide charge-neutral

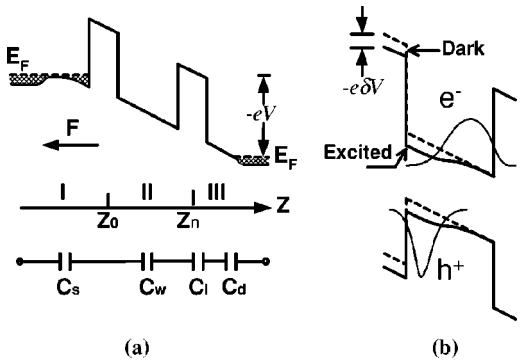

FIG. 1. (a) Schematic of the conduction-band edge of the DBS under forward bias. (b) Band-bending effect due to the displacement of electron and hole wave functions in the QW under applied field.

region (II), which makes the DBS behave like a capacitor with one electrode represented by the accumulation region and the other by the depletion region. The capacitance can then be defined in the form $C=dQ_s/dV$, where dQ_s denotes the difference of the stored charge associated with dc bias, induced by a small probe voltage dV.

Following Ref. 16, the total capacitance of the structure could be expressed as

$$C^{-1}=C_s^{-1}+C_I^{-1}+C_d^{-1}+C_w^{-1}. \tag{1}$$

Here C_s is the capacitance of a two-dimensional electron gas accumulating in the trianglelike potential well on the incident side. C_I is simply a series of the insulating layer capacitances of the two barriers, as well as the spacer on the outgoing side. C_d is the capacitance of the depletion layer. C_w, in which we are interested, represents the contribution from the central QW.

Under dark conditions, there is no free carrier accumulating in the central well, so that it acts just as an insulator. Consequently, the dark capacitance $C_{w,dark}$ of the central well is merely determined by its geometric capacitance. When a laser excitation of proper wavelength and power is continuously shined on the structure, a certain number of electrons and holes will be generated in the QW. We will only concentrate on the most typical and important case, where the electron and hole relaxation rates are much larger than the recombination rate. This places the electrons and holes inside the QW in quasiequilibrium states, respectively. At zero bias, the electrons and holes distribute symmetrically in the well, while this symmetry will be easily destroyed by an external electric field perpendicular to the QW, for the reason that the electron and hole envelope wave functions are displaced in opposite directions toward their respective potential minima [see Fig. 1(b)]. Owing to such a screening effect, upon excitation the potential drop across the central well $V_{w,exc}$ is lowered by an amount of δV with respect to $V_{w,dark}$ under dark conditions:

$$V_{w,exc}=V_{w,dark}-\delta V. \tag{2}$$

As the negative and positive charges overlap with each other in space, a classical treatment of the polarization of the dielectrics is no longer valid. Instead of the semiclassical theory employed in a previous work of Rosencher *et al.*[17] we here have performed a full quantum analysis based on the Hartree self-consistent model,[18] and δV can be carried out by directly integrating the Poisson equation,

$$\delta V=\int_{Z_0}^{Z_n}dz\left[\frac{q}{\epsilon_0\epsilon(z)}\int_{Z_0}^{z}dz'[p(z')-n(z')]\right], \tag{3}$$

where $n(z)$ and $p(z)$ denote the self-consistent electron and hole density in the well, respectively; q is the elementary charge; ϵ_0 the vacuum permittivity; and $\epsilon(z)$ the position-dependent dielectric constant. The integral limits Z_0 and Z_n, are taken sufficiently deep in the barriers where both electron and hole wave functions have vanished. The two-dimensional electron density may be written as

$$n(z)=\sum_{ie}\frac{m_e^* k_B T}{\pi\hbar^2}\ln\left\{1+\exp\left[\frac{E_{fe}-E_{ie}}{k_B T}\right]\right\}|\Psi_{ie}(z)|^2, \tag{4}$$

where m_e^* is the effective electron mass, k_B is Boltzmann's constant, T is the absolute temperature, $\hbar$ is Planck's constant divided by 2π, E_{ie} and Ψ_{ie} are the eigenenergy and the corresponding envelop wave function of the ieth electron subband, and E_{fe} is the quasi-Fermi-level determined by the sheet density of the electrons in the QW. Similarly we have a hole density in the form

$$p(z)=\sum_{ih}\frac{m_h^* k_B T}{\pi\hbar^2}\ln\left\{1+\exp\left[\frac{E_{fh}-E_{ih}}{k_B T}\right]\right\}|\Psi_{ih}(z)|^2, \tag{5}$$

where only the heavy-hole subbands have been taken into account. Differentiating Eq. (2) with respect to Q_s, we obtain the reciprocal value of the capacitance $C_{w,exc}$ in the form

$$C_{w,exc}^{-1}=C_{w,dark}^{-1}-C_Q^{-1}, \tag{6}$$

where we define

$$C_Q^{-1}=\frac{d(\delta V)}{dQ_s}. \tag{7}$$

Since Q_s is proportional to the external field applied on the QW as determined by Gauss's law, from Eqs. (3)–(7) it is clear that C_Q actually represents a quantum contribution to the capacitance originating from the polarization of nonlocal electron and hole wave functions, and directly reflecting the quantum-confined Stark effect.

It should be pointed out that a change in the voltage drop across the central well (region II) by the optical excitation is in turn going to cause a corresponding potential redistribution in the rest parts (I and III) in order to maintain the total dc bias constant. However, we can safely assume that the capacitances C_s, C_I, or C_d remain unchanged, since δV is very small under typical excitation, especially near zero bias. Under the above assumption, if we use C_{dark} and C_{exc} to denote the total capacitance of the DBS under dark and illumination conditions, respectively, from Eqs. (1) and (6) we obtain that

$$C_{dark}^{-1}-C_{exc}^{-1}=C_Q^{-1}. \tag{8}$$

One can explicitly extract the quantum component of the capacitance, C_Q, from experimentally measurable quantities C_{dark} and C_{exc}.

Based on Eqs. (3)–(7), we have performed numerical simulations of the quantum capacitance by solving the Schödinger equation and the Poisson equation self-consistently. The average sheet density of the two-dimensional electron or hole gas (N_{eh}) in the QW, which is assumed not to vary with bias, was taken as a parameter in the simulation. Both Schödinger and Poisson equations were solved with the finite-difference method. For convenience, the DBS has been divided into three separate regions, with the middle planes of the barriers as the boundaries [see Fig. 1(a)]. The field continuity at each boundary between adjacent

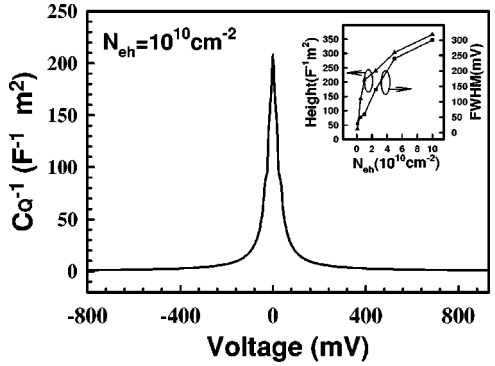

FIG. 2. Self-consistently simulated reciprocal quantum capacitance vs voltage ($C_Q^{-1}-V$) characteristic at 4.2 K. The average sheet density of electron or hole gas (N_{eh}) in the QW is assumed to be 10^{10} cm^{-2}. Shown in the inset are the FWHM and height of the simulated reciprocal quantum capacitance peak as functions of the sheet density N_{eh}.

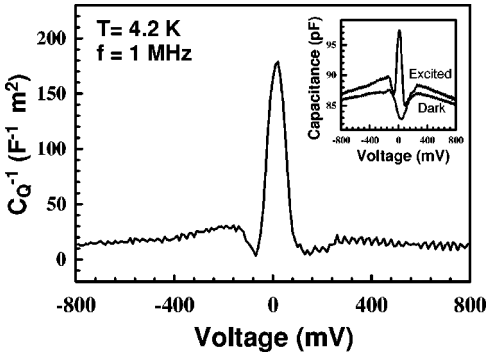

FIG. 3. Measured $C_Q^{-1}(V)=C_{dark}^{-1}(V)-C_{exc}^{-1}(V)$ at a temperature of 4.2 K upon Ti-sapphire laser excitations of $\lambda=800$ nm and $P\sim 10$ μW. Shown in the inset are experimental C_{exc}-V and C_{dark}-V characteristics.

regions is ensured. For a given total charge Q_s, and correspondingly a given field taken as the boundary condition for the Poisson equation, iterations were performed individually in each region until the potential profile and charge density converged.[9] Then the voltage across the whole structure V was obtained by simply adding up the potential drop across each region. The screened potential drop δV was also evaluated from the obtained self-consistent charge density by using Eq. (3). Knowing the potential drops V and δV for a set of mesh points of the total charge Q_s, the quantum capacitance as a function of applied voltage was finally derived from the derivative defined in Eq. (7).

Shown in Fig. 2 is the calculated reciprocal quantum capacitance vs voltage curve ($C_Q^{-1}-V$) for a fixed N_{eh} of 10^{10} cm^{-2} at a temperature of 4.2 K. The sharp peak at zero bias features the simulation result, signaling a prominent Stark effect in a wide QW. In this case even relatively weak electric fields can induce a strong deformation of the rectangular potential well. With increasing bias either positively or negatively, the overlap between the electron and hole wave functions is dramatically decreased, which causes C_Q^{-1} or $C_{w,exc}$ to have a maximum under zero bias. With further increasing bias, the relative shift of electron and hole wave functions slows down and eventually saturates, and C_Q^{-1} correspondingly declines to zero.

To experimentally examine the above prediction, the wafer was processed into rectangular mesas (650×350 μm^2) using standard photolithography. The top contact was fabricated by evaporating and subsequently alloying Au/Ge/Ni onto the cap layer through a pattern with a square aperture (300 μm) left for illumination. The rear contact was formed by alloying In to the n^+-GaAs substrate. During the experiments, the sample was immersed in liquid helium. The C-V measurements were carried out on a Hewlett-Packard 4284A LCR meter with a modulation frequency of 1 MHz and an amplitude of 10 mV. A Ti-sapphire laser with a wavelength of 800 nm and a weak power of $\sim$10 μW was used for excitation.

The measured C-V spectra with and without photoexcitation are shown in the inset to of Fig. 3. In sharp contrast to the result of Rosencher *et al.*,[17] where the photocapacitance showed a dip near the zero bias, a capacitance peak instead grows up with illumination around zero bias. By simply using Eq. (8), we extracted the quantum component of the reciprocal capacitance, and illustrated it in Fig. 3. The experimental result of the C_Q^{-1}-V characteristic agrees fairly well with the theoretical one, except that the peak is somewhat broadened.

However, there are still several remarks we should address. One should be aware that a constant sheet density of electron or hole gas (N_{eh}) in the QW, as assumed in the calculation, is actually not valid in the experiment, when the bias scans away from the zero voltage. The electric field applied across the QW not only gives rise to a polarization of electron and hole wave functions in space, but also reduces the optical recombination rate. Since the photocarrier concentration is determined by the balance between the optical generation and electron-hole recombination, it should be increasing with the bias. One has to check the possible influence of a bias-dependent sheet density N_{eh} on the C_Q^{-1}-V curve. It follows from our simulations that a higher sheet density results in a broader and stronger peak in the C_Q^{-1}-V curve, but does not destroy this quantum feature. For clarity, we have plotted the full width at half maximum (FWHM) and height of the C_Q^{-1} peak as functions of N_{eh} in the inset to Fig. 2. Judged from the experimental curve in Fig. 3, the corresponding carrier sheet density should not exceed 1.5 $\times10^{10}$ cm^{-2} in a bias range where there is significant photoresponse. Whereas the increase in C_Q^{-1}, induced by such an enhancement in the carrier concentration, is rather slight, as verified theoretically (see the inset to Fig. 2), which coincides well with the slightly broadened peak feature observed in the experiment. Thus one has a good reason to believe that the assumption of a fixed average sheet density in the theoretical simulation is still an efficient approximation in the present case. Second, by measuring the bias dependence of the photoluminescence (PL) intensity I_{PL} of the QW, we found a much broadened peak in the I_{PL}-V curve with a FWHM of 400 mV in comparison to the 80-mV FWHM of the reciprocal photo capacitance peak. Accordingly we are

convinced that the quantum capacitance observed here in the photo capacitance vs voltage curve in a sense more truly reflects the quantum-confined Stark effects. Finally, the possible accumulation of photon-generated holes at the interface between the AlAs barrier and the GaAs spacer adjacent to the depletion region has not been taken into account. As can be inferred from the experimental data, under our experimental conditions (weak illumination and small biases) such an effect is neglectable. If this is not the case, there should appear a significant asymmetry in the photocapacitance curve, as the laser is always injected from the surface of the sample and correspondingly the density of the photo generated hole gas depends on whether the sample is positively or negatively biased.

In conclusion, we have investigated the capacitance characteristics associated with the optically excited electron and hole gas in a wide QW. A unique capacitance peak grows up with illumination around zero bias, in direct response to the spatial displacement of electron and hole wave functions with the applied field, and has thus been considered as an electrical manifestation of the quantum-confined Stark effect. A comparison between the result of a selfconsistent simulation and that of experiment shows fairly good agreement, unambiguously verifying the above claim.

The authors wish to thank Xiaoguang Wu for stimulating discussions concerning the theoretical calculations. This work was supported by the State Council of Science and Technology, and National Natural Science Foundation of China (NSFC) through Contract No. 19734002.

*Email: ytang@red.semi.ac.cn

[1] H. Drexler, D. Leonard, W. Hansen, J.P. Kotthaus, and P.M. Petroff, Phys. Rev. Lett. **73**, 2252 (1994).
[2] R.C. Ashoori, H.L. Stormer, J.S. Weiner, L.N. Pfeiffer, S.J. Pearton, K.W. Baldwin, and K.W. West, Phys. Rev. Lett. **68**, 3088 (1992).
[3] R.J. Warburton, C.S. Dürr, K. Karrai, J.P. Kotthaus, G. Medeiros-Ribeiro, and P.M. Petroff, Phys. Rev. Lett. **79**, 5282 (1997).
[4] A.J. Chiquito, Yu.A. Pusep, S. Mergulhão, and J.C. Galzerani, Phys. Rev. B **61**, 5499 (2000).
[5] T. Jungwirth and L. Smrčka, Phys. Rev. B **51**, 10 181 (1995).
[6] S. Luryi, Appl. Phys. Lett. **47**, 490 (1985).
[7] Y.M. Hu and S. Stapleton, Appl. Phys. Lett. **58**, 167 (1991).
[8] S. Luryi, Appl. Phys. Lett. **59**, 2335 (1991).
[9] T. Wei and S. Stapleton, Solid-State Electron. **38**, 465 (1995).
[10] T. Wei and S. Stapleton, J. Appl. Phys. **76**, 1287 (1994).
[11] A. Kindlihagen, A.G. Mal'shukov, K.A. Chao, and M. Willander, Phys. Rev. B **58**, 10 602 (1998).
[12] S. Luryi, Appl. Phys. Lett. **52**, 501 (1988).
[13] Y.H. Zhang, Y.X. Li, D.S. Jiang, X.P. Yang, and P.H. Zhang, Appl. Phys. Lett. **64**, 3416 (1994).
[14] K. Fobelets, R. Vounckx, J. Genoe, G. Borghs, H. Grönqvist, and L. Lundgren, Appl. Phys. Lett. **64**, 2523 (1994).
[15] M.E. Lazzouni and L.J. Sham, Phys. Rev. B **48**, 8948 (1993).
[16] H.Z. Zheng, A.M. Song, F.H. Yang, and Y.X. Li, Phys. Rev. B **49**, 1802 (1994).
[17] R. Rosencher, N. Vodidani, J. Nagle, P. Bois, E. Costard, and S. Delaitre, Appl. Phys. Lett. **55**, 1853 (1989).
[18] W.R. Frensley, Solid-State Electron. **32**, 1235 (1989).